Hydrophobic surface modification of membrane distillation (MD) membranes using water-repelling polymer based on urethane rubber

Jungwoo Jung[a], Yonghyun Shin[a], Yong-Jun Choi[a], Jinsik Sohn[a], Sangho Lee[a,*], Kyoungjin An[b]

[a]*School of Civil and Environmental Engineering, Kookmin University, Seoul, Korea, Tel. +82 2 910 4529; Fax: +82 2 910 4939; email: sanghlee@kookmin.ac.kr (S. Lee)*
[b]*School of Energy and Environment, City University of Hong Kong, Kowloon, Hong Kong*

ABSTRACT

Membrane distillation (MD) is a unit process that uses hydrophobic membranes to separate vapor from saline water. The performance of the MD process is largely affected by the properties of the membranes, which should be porous, hydrophobic, and stable under high temperature conditions. Accordingly, it is essential to develop highly efficient membranes for practical implementation of MD technology. In this study, we applied a water repellent chemical (WRC) made of urethane rubber onto hydrophilic membranes to develop a novel approach for MD membrane preparation. A spin coating method was adopted to introduce hydrophobic coating layers on polyamide membranes. Experiments were carried out in the direct contact membrane distillation mode. Contact angle and liquid entry pressure (LEP) were measured before and after the surface coating. In addition, scanning electronic microscope, FT-IR, and atomic force microscope analysis were conducted to confirm a coating layer of the membrane. The optimum condition for the spin coating was 1,500 rpm for 20 s and flux, rejection, and LEP were 6.78 kg/m^2-h, 99.9%, and 1.65 bar, respectively. These results confirmed that the membranes prepared by the surface coating of WRC have potential for use in MD process.

Keywords: Water-repelling chemical; Urethane rubber; Membrane distillation; Surface modification; Liquid entry pressure; Flux; Rejection

1. Introduction

Membrane distillation (MD) is a separation process using a vapor pressure, which is caused by the temperature difference of surfaces contacted feed and permeate water [1]. MD process has advantages over conventional technologies, including the ability of treating highly concentrated feed water and less stringent requirement of pretreatment [2]. If waste heat occurred from an electronic power station or solar heat energy is used at MD process, energy consumption will be reduced rather than current RO process. Moreover, the MD process can be used as a hybrid process with

---

*Corresponding author.

bioreactor (MD-MBR) [3–5]. Therefore, MD process has potential as an alternative technology for seawater desalination [6].

Since the membrane controls heat and mass transfer in MD, the efficiency of the MD process is governed by the characteristics of the membranes. The MD membranes should be porous, hydrophobic, resistant to heat conduction, and affordable. However, current membrane materials, which are based on polypropylene or fluoropolymer, have limited properties and are relatively expensive [7,8]. Accordingly, a few studies have been done for the development of new membrane materials for MD process [9].

Surface modification is one of the approaches for developing novel MD membranes [10–12]. For example, a plasma treatment is widely used for modifying the surface properties of the membranes, which is effective to form hydrophobic layer. However, the plasma treatment is relative expensive and requires a special equipment, which make it difficult to scale up. Accordingly, a simple and affordable method is required for surface modification. Spin coating is a convention technique, which is easy to implement [13]. The formation of the coating layer can be readily controlled by adjusting the operating parameters. Thus, the combination of the spin coating with an appropriate coating materials may be an alternative approach for membrane surface modification [14].

This study describes the results of surface modification by a spin coating method. A water repellent chemical (WRC) based on urethane rubber was used. It is relatively inexpensive, non-toxic, and environmentally friendly. A series of direct contact membrane distillation (DCMD) was attempted to examine the performance of the prepared membranes. Contact angle (CA) and liquid entry pressure (LEP) for the prepared membranes were measured. Surface analysis such as scanning electronic microscope (SEM), FT-IR, and atomic force microscope (AFM) were also conducted to characterize the prepared membranes.

2. Materials and methods

2.1. Water repellent chemical

A WRC is used to form the hydrophobic layer on top of the interlayer. It is based on material mixed hydrogenated styrene-butadiene polymer (SBR) and dimethyl ether in solvent naphtha. At this time, the hydrogenated SBR makes hydrophobic film after solvent naphtha and dimethyl ether were volatilized and reacted with SBR [15,16]. So, the repellent chemical (WRC) helps a membrane surface to make super-hydrophobic. It is available to coat inner side

Table 1
Characteristic of the WRC

Properties item	Result
Appearance	Clear liquid
Color, APHA	86
Viscosity (25℃), cPs	8.73
Specific gravity (25℃)	0.65–0.80

and have high porosity of membrane surface. There are the characteristic and the chemical composition of WRC in Tables 1 and 2.

2.2. Membrane

Hydrophilic polyamide (PA) membrane fabricated by "WHATMAN" was used to modify membrane surface hydrophobicity in this study. It has pore size of 0.45 μm, and its thickness is 110 μm. Polyvinylidene fluoride (PVDF, 0.45 μm) and polypropylene (PP, 0.45 μm) membrane were also adopted to compare the performance of the modified membrane.

2.3. Membrane surface modification

A coating method of many surface modification technologies was adopted in this study. The membrane surface was covered with WRC using the spin coater (EF-40P, E-Flex, South Korea) to produce a uniform layer with the control of the coating thickness. The rotating rate of the spin coater for WRC was 1,500 rpm for 20 s, leading to the formation of the most excellent membrane. However, the rotating speed gradually increases in 500 rpm for 5 s. After this process, the membrane was secondly coated by WRC and dried at room temperature for 24 h.

2.4. Membrane characterization

2.4.1. Scanning electronic microscope (SEM)

The structures of coating layer on the membrane surface were investigated by field emission scanning electron microscopy (Model: S-4700, Hitachi, Japan). Before coating membrane with platinum, samples were completely dried at 60℃ for 2 h in a dry oven. And membrane samples were coated with platinum for 110 s by sputtering.

2.4.2. Atomic force microscope (AFM)

AFM (Model: MFP-3D, Asylum Research, USA) images of the top membrane surfaces were obtained

Table 2
Chemical composition of the WRC

Chemical name	CAS number	Content (%)
Solvent naphtha (petroleum)	64,772-89-8	40–70
Dimethyl ether	115-10-6	15–40
Hydrogenated styrene-butadiene polymer	66,070-58-4	5–15

over each surface using tapping mode. The procedure to take the AFM images has been described elsewhere [17]. The same tip was used to scan both membrane surfaces, and all captured images were treated in the same way.

The root mean square (RMS) roughness and the average roughness (R_a) were determined using the same scan size (5 μm × 5 μm). Average roughness is defined as the average deviation of the peaks and valleys from the mean plane, and RMS roughness is the RMS deviation of the peaks and valleys from the mean plane.

2.4.3. Fourier transform infrared spectroscopy (ATR-FTIR)

ATR-FTIR was used to verify the formation of coating layer from a WRC on the raw PA membrane surface. A modified membrane was compared with a raw membrane by ATR-FTIR analysis, and it could confirm the type of formed functional groups. Attenuated total reflectance methods penetrate the light, which penetrating depth is approximately 0.5–2 μ. It is broadly detected not only surface, but also internal membrane.

2.4.4. Contact angle

CAs on the membrane surface were measured by a contact angle meter (Model: DSA 100, KRÜSS, Germany). A water droplet of 5 μL was deposited on the membrane surface at 25℃, and contact angles of a membrane sample were measured 5 times. Its images and average values were analyzed by a high speed CCD camera and goniometer software.

2.4.5. Liquid entry pressure

LEP is widely used to measure the ability of hydrophobic membrane against pore wetting. A device measuring LEP was consist of a dead-end filtration style and used deionized water as a solvent for the measurement. Pressure on the feed water side was increased step by step (each increment: 0.1 bar) with

confirming first water droplet on the membrane surface for holding times (about 5 min). LEP is the pressure when first water droplet was measured.

2.4.6. Thermal conductivity

Thermal conductivity of a membrane is examined to confirm heat loss in MD process. Therefore, thermal conductivity of hydrophobic membrane is very important in the membrane development research for MD process. Thermal conductivities of the membranes were measured by thermal diffusivity measurement equipment (Model: LFA 447 NanoFlash, NETZSCH, Germany). The standard test method for thermal diffusivity by the flash method (ASTM E1461) was adopted. Thermal conductivity was calculated by Eq. (1).

$$\lambda(T) = \alpha(T) \times C_p(T) \times \rho(T) \tag{1}$$

where α is the thermal diffusivity, C_p is the specific heat, and ρ is the density of the membrane. Operation of the experiment was conducted at 25℃.

2.5. DCMD experiment

A laboratory-scale flat-sheet membrane cells were used for DCMD. A schematic diagram describing the experimental setup is shown in Fig. 1. The deionized water and sodium chloride (NaCl) solution (3.5 wt%) were respectively used as the permeate and the feed water. The permeate water was deionized water. To maintain a constant feed water concentration, additional deionized water was added based on the amount of water transferred across the membrane.

The feed temperature was varied in the range of 50–70℃ and the permeate temperature was maintained at 20℃. Variable speed gear pumps (Micropump, Vancouver, WA) were used to pump feed and permeate water. A pump of feed side was operated in the range of 200–600 mL/min, and the other was used to maintain a flow rate of 200 mL/min. There are detailed experimental conditions in Table 3. The permeate water was collected as an over flow and
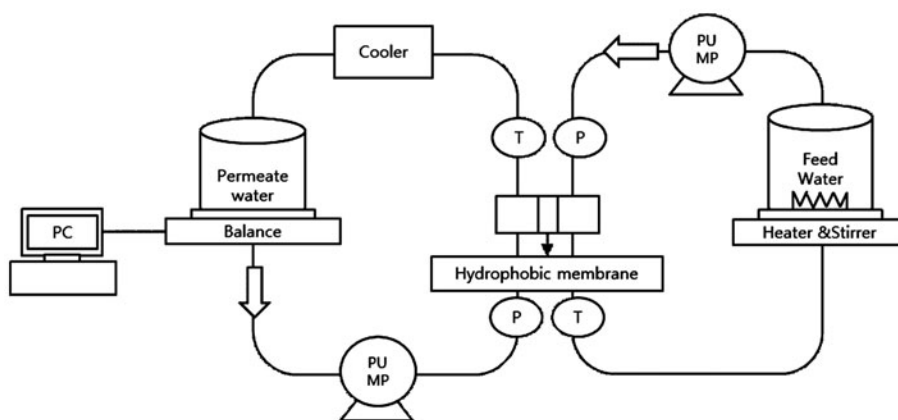
Fig. 1. Schematic diagram of experimental set-up for DCMD test.

Table 3
Experimental conditions of DCMD

	Experimental condition
Feed type	Deionized water, NaCl 35,000 ppm
Permeate type	Deionized water
Feed temperature (℃)	50–70
Permeate temperature (℃)	20
Feed flow rate (ml/min)	200–600
Permeate flow rate (ml/min)	200
Feed/permeate volume (L)	2/1.5

continuously monitored by an electronic balance connected to a personal computer.

3. Results and discussion

3.1. Optimization of spin coating condition for WRC coating

A spin coater was used to apply the water repellent material on the membrane surface. This membrane was evaluated in the MD experiment test. The feed and permeate temperature were 50 and 20℃, respectively. A NaCl solution (35 g/L) was used as the feed water, and rejection rate was analyzed by conductivity meter. Table 4 and Fig. 2 show the average flux, LEP, and rejection of membranes coated under various conditions of rotational speeds (from 1,500 to 3,000 rpm) and coating time (from 5 to 20 s). It is interesting to note that the flux decreased as the rotational speed increases. Accordingly, the membrane prepared at 1,500 rpm showed highest flux and reasonable LEP and salt rejection, implying that this is the optimum condition. The LEP was improved as an increase in coating time, and the rejection was almost constant at 99%. Based on these results, the spin coating under the condition of 1,500 rpm and 20 s was determined to be the optimum conditions for WRC coating. Under this condition, the flux and LEP were 3.28 kg/m^2-h and 1.65 bar, respectively.

3.2. Membrane characterization

3.2.1. Morphology of the modified membrane

The surface morphology of the membranes was examined before and after coating of membrane surfaces. In this analysis, two membranes were compared: (i) an original membrane (base membrane) and (ii) a membrane coated by the WRC. Fig. 3(a) shows the base membrane, which has open and rough surface structure. After applying the WRC to the membrane surface, it showed a different structure. As shown in the SEM image of Fig. 3(b), the fabric structure coated by the WRC could be confirmed and became thick rather than base membrane. This coating layer plays an important role in active layer as hydrophobic membrane.

Table 4
Membrane performance according to the RPM velocity of WRC

| Number	Operation condition	Average flux	LEP	Rejection rate
#1	1,500 rpm 10 s	3.44	1.30	99.79
#2	2,000 rpm 10 s	3.09	1.35	99.92
#3	2,500 rpm 10 s	2.67	1.35	99.79
#4	3,000 rpm 10 s	1.09	1.26	99.47
#5	1,500 rpm 15 s	2.28	1.38	99.63
#6	2,000 rpm 15 s	0.22	1.45	99.92
#7	2,500 rpm 15 s	0.88	1.45	99.79
#8	3,000 rpm 15 s	0.54	1.30	99.47
#9	1,500 rpm 20 s	3.28	1.65	99.84
#10	2000 rpm 20 s	3.01	1.57	99.85
#11	2,500 rpm 20 s	1.53	1.55	99.35
#12	3,000 rpm 20 s	1.64	1.40	99.99
#13	1,500 rpm 25 s	2.41	1.50	99.76
#14	2,000 rpm 25 s	3.01	1.35	99.96
#15	2,500 rpm 25 s	3.17	1.50	99.73
#16	3,000 rpm 25 s	0.90	1.50	99.85
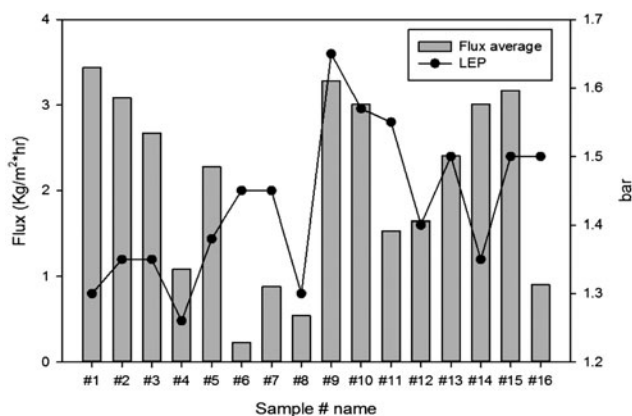
Fig. 2. The performance assessment of membranes coated by WRC.

3.2.2. Roughness of the modified membrane

AFM was applied to analyze the surface structures of the base membrane and the modified membrane. Fig. 4 shows the AFM images for the membranes. The values of surface roughness for all the membranes are listed in Table 5. Here, the average roughness is defined as the average deviation of the peaks and valleys from the mean plane, and the RMS roughness is the RMS deviation of the peaks and valleys from the mean plane. Both average roughness (R_a) and RMS sharply increased by the coating. When the WRC was used for surface coating, the roughness of the membrane surface is higher than that of the base membrane. This suggests that the surface morphology of the membrane coated by WRC is different from base membrane.
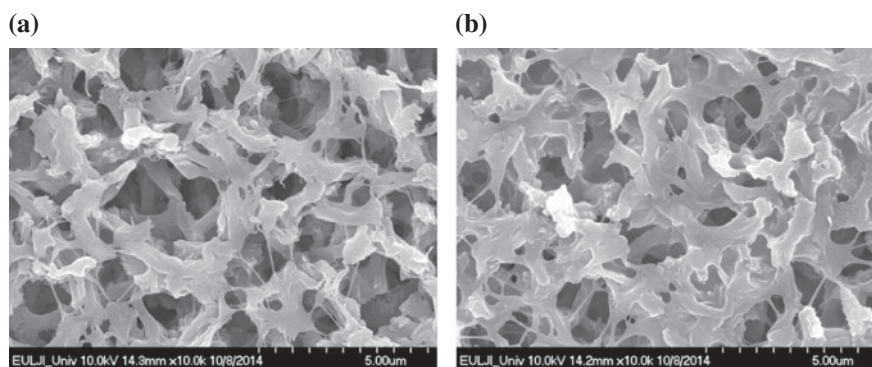
(a)   **(b)**

Fig. 3. Surface SEM images of modified PA membrane. (a) Base membrane and (b) membrane coated by WRC.
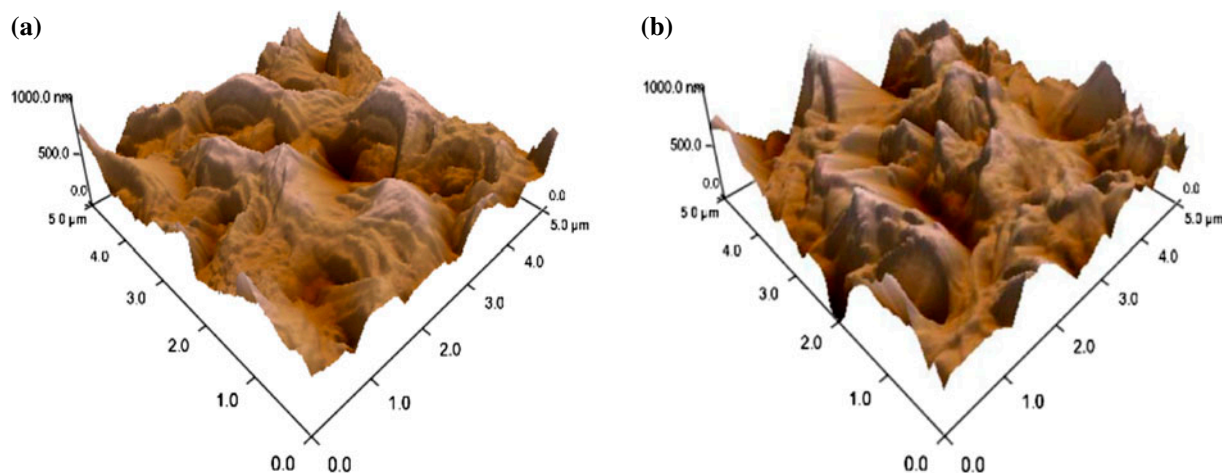
(a)

(b)

Fig. 4. AFM images of the modified membrane and the others. (a) Base membrane and (b) membrane coated by WRC.

Table 5
Roughness values of the modified membrane and the others

	Base	WRC
RMS (nm)	119.9	132.0
R_a (nm)	95.5	103.4

3.2.3. FTIR analysis

Chemical structures of the membrane before and after modification were examined by ATR-FTIR, and results are illustrated in Fig. 5. This study was conducted to analyze the chemical structure of the support membrane, the coating membrane. The peaks here are characteristic for the water proof polymer. As the coating layer formed, the intensity of the peaks increased. As shown in Fig. 5, they are slightly different at the aspect of %T, but all have same peaks in FTIR analysis. For the modified membrane coated by WRC, the pair of features at 2,926 and 2,854 cm^{-1} is characteristic of the C-H2 symmetrical and asymmetrical stretching vibrations in aliphatic hydrocarbons. Moreover, the pair of features at 3,300 cm^{-1} is characteristic of the C–H. H2O is also characterized by a bending mode at 1,632 cm^{-1} [7,18]. These values are between the result of the membrane coated by WRC and base. So, it could confirm that the modified membrane was well coated.

3.2.4. CA of the modified membrane

Table 6 compares the contact angles for the membranes before and after coating. The contact angles of other hydrophobic membranes were also summarized. It appears that the membranes coated by WRC have similar CA to PVDF membranes. On the other hand, the base membrane showed the CA of 0° because it was completely wetted. Fig. 6 shows the CA images for various membranes.

3.2.5. LEP of the modified membrane

Table 7 summarizes the LEP for the membranes before and after coating and for other hydrophobic membranes. The membrane coated by WRC resulted in the LEP of 1.65 bar, which is acceptable for MD operation.

Although these LEP values are lower than those for the PVDF and PTFE membranes, they are still suitable for MD process such as VMD, SGMD, AGMD, and so on. Moreover, these LEP values are much higher than that of the base membrane because the base membrane is immediately wetted by water and hydrophobic coating layer was formed.

3.2.6. Thermal conductivity of the modified membrane

Table 8 summarizes the thermal conductivity for the modified membranes and other commercial membranes. The membrane coated by WRC resulted in the thermal conductivity of 1.45 W/m-k, which is acceptable for MD operation. Also, this membrane has lower thermal conductivity than other commercial membranes. Therefore, this membrane can help to reduce energy consumption and cost because of low heat loss from membrane surface [19].
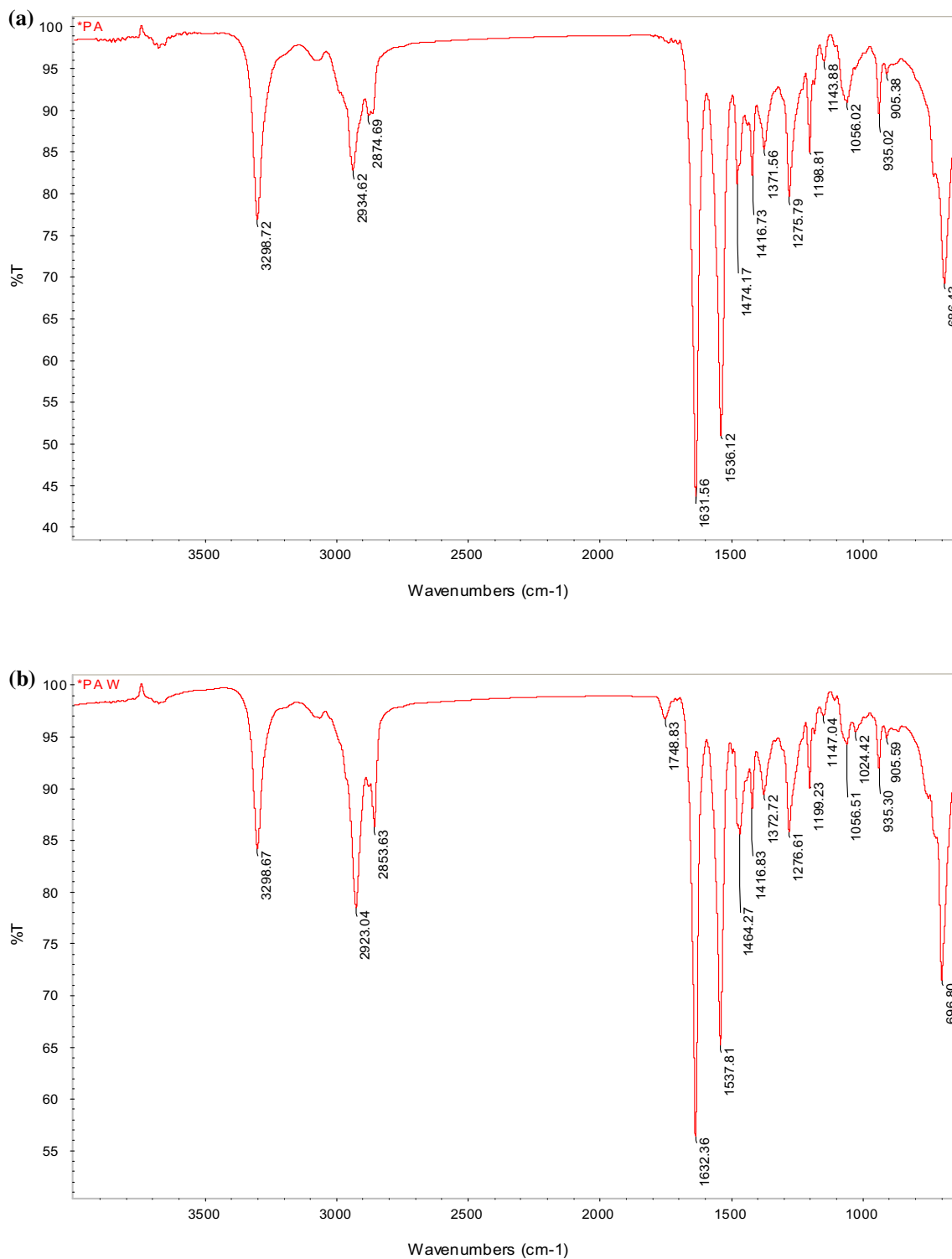
Fig. 5. FT-IR analysis images of the modified membrane and the others. (a) Base membrane and (b) membrane coated by WRC.

Table 6
CA value of the modified and commercial membranes

	CA (°)
PP membrane (0.45 μm)	134.5
PVDF membrane (0.45 μm)	122.3
Membrane coated by WRC (0.45 μm)	126.6
Base membrane (0.45 μm)	0

Table 7
LEP value of the modified and commercial membranes

	LEP (bar)
Base membrane	0
Membrane coated by WRC	1.65
PP membrane	2.6
PVDF membrane	2.4

3.3. Performance of the modified membrane in DCMD

3.3.1. Performance comparison with commercial membrane

Fig. 7 compares the flux and salt rejection for the modified membranes and commercial hydrophobic membranes. All the tests were done in DCMD mode. The feed temperature was 60℃, and the permeate temperature was 20℃. The flux for the modified membrane was 6.78 kg/m^2-h, which were 30% of the flux for the commercial PP membrane (22.8 kg/m^2-hr) at feed condition of NaCl solution. However, the rejection for the modified membrane was similar to those for the PP membranes.

Table 8
Thermal conductivity of the modified and commercial membranes

	Thermal conductivity (W/m-k)
Membrane coated by WRC	1.45
PTFE membrane	2.49
PVDF membrane	2.25

Although the flux for the modified membrane is lower than those for the hydrophobic membranes, it should be noted that this surface modification technique has potential to enable the use of
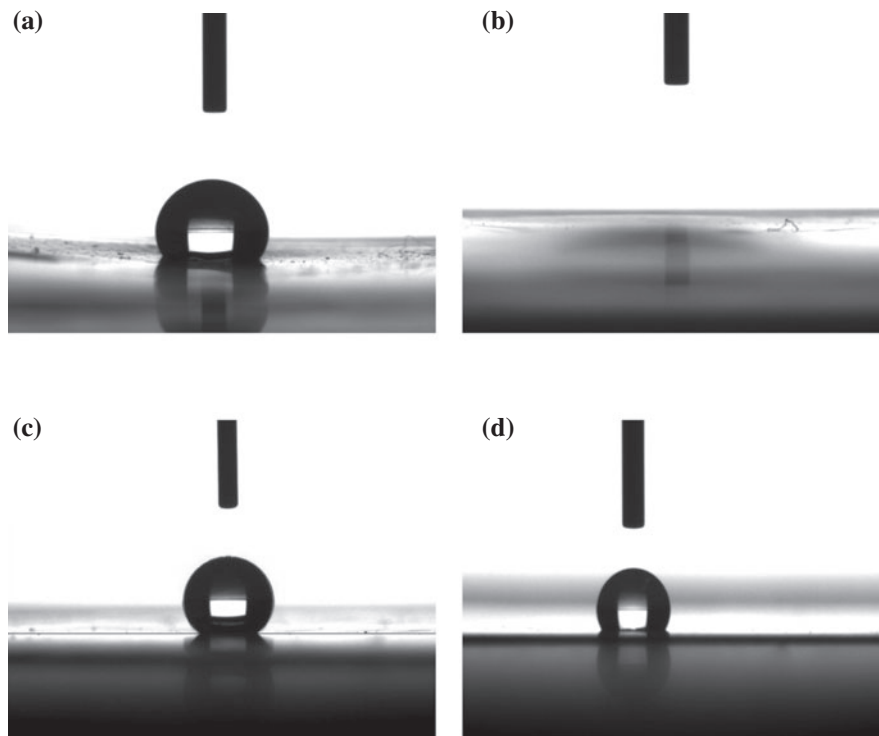

Fig. 6. CA images of the modified and commercial membranes (a) membrane coated by WRC, (b) Base membrane, (c) PP membrane, and (d) PVDF membrane.
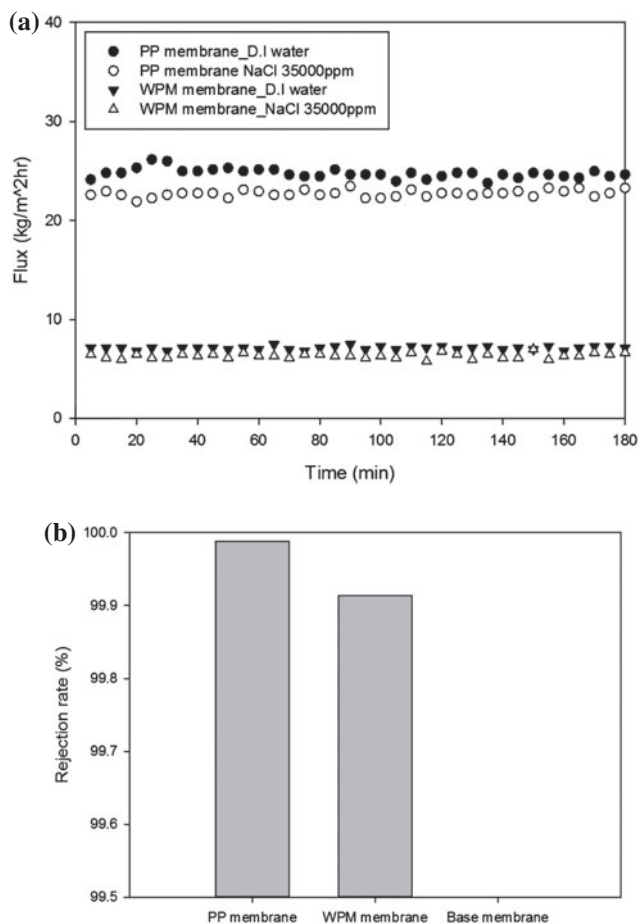
Fig. 7. Comparison of (a) flux and (b) rejection rate with commercial membrane.

Fig. 8. Comparison of (a) flux and (b) rejection rate at different feed temperatures.

membranes made of cheaper materials. Moreover, this technique allows the use of membranes made of various polymeric materials.

3.3.2. Effect of feed temperature on performance of modified membranes

Using the modified membrane, the effect of feed temperature on the flux and salt rejection was investigated. The feed temperature was adjusted from 50 to 70°C. Both distilled water and NaCl solution (35 g/L) were used as the feed water. As shown in Fig. 8, the flux increases from 5 to 17 kg/m²-h as the feed temperature increased from 50 to 70°C at feed condition of distilled water. The rejection was over 99% for all conditions although the rejection at 50°C was slightly lower than the other cases. According to the Antoine equation, the vapor
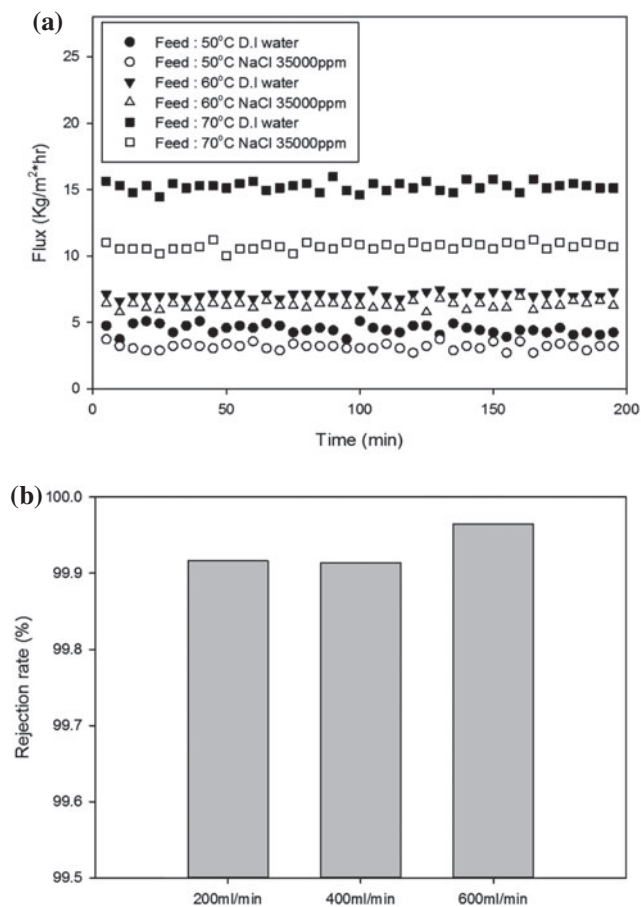
pressure increases exponentially with temperature. Therefore, the operating temperature has an exponential effect on the permeate flux [7]. Moreover, flux increases with an increase in feed temperature since temperature polarization decreases with increasing feed temperature [19,20].

3.3.3. Effect of feed velocity on performance of modified membranes

The effect of the feed velocity on the flux and rejection for the modified membranes were also investigated. For these experiments, the feed temperature was adjusted from 50 to 70°C. Both D.I water and NaCl solution (35 g/L) were used as the feed water.

As shown in Fig. 9(a), the flux increases with an increase in the feed velocity. This is attributed to an enhanced mixing in the flow channel and a decrease
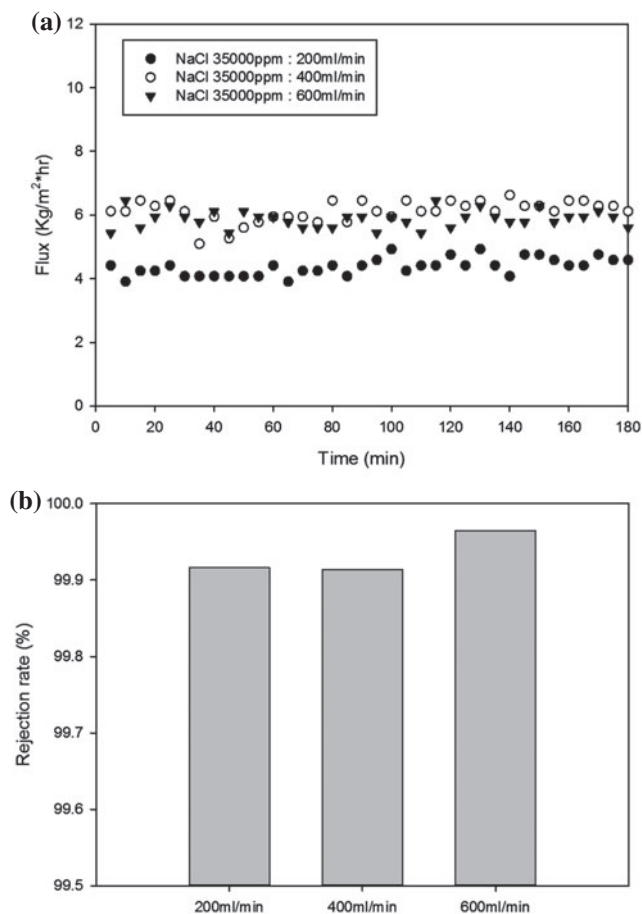
Fig. 9. Comparison of (a) flux and (b) rejection rate according to feed flow velocity.

Fig. 10. Comparison of (a) flux and (b) rejection in the long-term test.

in the thickness of the temperature boundary layer [21]. Moreover, an increase in the feed velocity results in high shear force, which limits the concentration polarization [22].

3.3.4. Membrane stability evaluation during long operation

The stability of the coating layer on the membrane surface is important for continuous MD operation. Accordingly, the performance of the modified membrane was examined for about 5 d using a NaCl solution of 35 g/L to confirm its stability. As illustrated in Fig. 10, the flux and salt concentration in permeate were maintained constant. The average flux was 7.57 kg/m²-h, and the salt rejection was over 99.99%. There was no sign of pore wetting and detachment of coating layer. It is evident from the results that this modified membrane has potential for long-term MD operation.
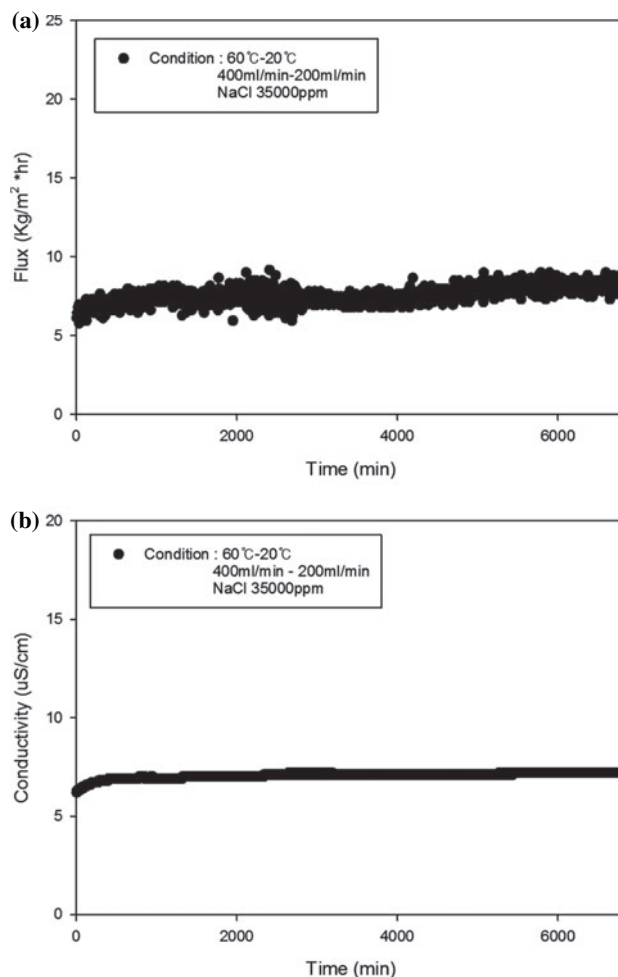
4. Conclusions

This study was conducted to develop a new hydrophobic coating membrane by applying a WRC through a spin coating method. Based on the results in this study, the following conclusions can be drawn:

(1) Spin coating was implemented for WRC coating under various conditions. The optimum condition was 1,500 rpm for 20 s, and this condition has the highest flux and LEP value to hydrophobic coating membrane in DCMD experiments. The modified membrane showed the flux of 6.78 kg/m²-h, the salt rejection of 99.9%, and the LEP of 1.65 bar, respectively. The feasibility of using the modified membrane for DCMD process was confirmed. This membrane has the stability without pore wetting in the long term.

(2) As the feed temperature increases, the flux and rejection for the modified membrane increase due to an increase in vapor pressure. With an increase in feed flow velocity, a reduction in temperature polarization by the hydrodynamic effect leads to an increase in the flux for the modified membrane.

(3) This modification technology was expected to increase the physical tensile strength from the formation of thick coating layer. Moreover, this membrane has lower thermal conductivity than other commercial membranes. Therefore, this membrane can help to reduce energy consumption and cost because of low heat loss from membrane surface.

(4) This modified membrane may be also used for not only DCMD but also VMD, AGMD, and SGMD because it has enough permeability and LEP value over 1.3 bar. Moreover, it also has potential to fix the damaged membrane from scratch and so on.

Acknowledgments

References

[1] A.G. Fane, R. Wang, C.Y. Tang, X. Yang, Membrane distillation and forward osmosis: Advances in membranes, modules, and applications, IDA J. Desalin. Water Reuse 4(1) (2013) 22–26.

[2] A. Alkhudhiri, N. Darwish, N. Hilal, Membrane distillation: A comprehensive review, Desalination 287 (2012) 2–18.

[3] X. Cui, K.H. Choo, Natural organic matter removal and fouling control in low-pressure membrane filtration for water treatment, Environ. Eng. Res. 19(1) (2014) 1–8.

[4] K. Lee, O.K. Choi, J.H. Song, J.W. Lee, Membrane diffuser coupled bioreactor for methanotrophic denitrification under non-aerated condition: Suggestion as a post-denitrification option, Environ. Eng. Res. 19(1) (2014) 75–81.

[5] S. Paudel, C.Y. Seong, D.R. Park, Anaerobic hydrogen fermentation and membrane bioreactor (MBR) for decentralized sanitation and reuse-organic removal and resource recovery, Environ. Eng. Res. 19(4) (2014) 387–393.

[6] W.T. Hanbury, T. Hodgkiess, Membrane distillation—An assessment, Desalination 56 (1985) 287–297.

[7] M.S. El-Bourawi, Z. Ding, R. Ma, M. Khayet, A framework for better understanding membrane distillation separation process, J. Membr. Sci. 285 (2006) 4–29.

[8] A. Burgoyne, M.M. Vahdati, Direct contact membrane distillation, Sep. Sci. Technol. 35 (2000) 1257.

[9] M. Son, H. Choi, L. Liu, H. Park, H. Choi, Optimized synthesis conditions of polyethersulfone support layer for enhanced water flux for thin film composite membrane, Environ. Eng. Res. 19(4) (2014) 339–344.

[10] Y. Wu, Y. Kong, X. Lin, W. Liu, J. Xu, Surface-modified hydrophilic membranes in membrane distillation, J. Membr. Sci. 72 (1992) 189–196.

[11] Y. Kong, X. Lin, Y. Wu, J. Chen, J. Xu, Plasma polymerization of octafluorocyclobutane and hydrophobic microporous composite membranes for membrane distillation, J. Appl. Polym. Sci. 46 (1992) 191–199.

[12] M. Peng, H. Li, L. Wu, Q. Zheng, Y. Chen, W. Gu, Porous poly(vinylidene fluoride) membrane with highly hydrophobic surface, J. Appl. Polym. Sci. 98 (2005) 1358–1363.

[13] L. Yan, K. Wang, L. Ye, Super hydrophobic property of PVDF/CaCO$_3$ nanocomposite coatings, J. Mater. Sci. Lett. 22 (2003) 1713–1717.

[14] H. Chang, J.-S. Liau, C.-D. Ho, W.-H. Wang, Simulation of membrane distillation modules for desalination by developing user's model on Aspen Plus platform, Desalination 249 (2009) 380–387.

[15] B. Arkles, Hydrophobicity, hydrophilicity and silanes, Gelest Inc., Paint Coatings Ind. Mag. (10) (2006) 114–132.

[16] R.V. Lapshin, A.P. Alekhin, A.G. Kirilenko, S.L. Odintsov, V.A. Krotkov, Vacuum ultraviolet smoothing of nanometer-scale asperities of poly(methyl methacrylate) surface, J. Surf. Investig. X-ray, synchrotron and neutron techniques. Pleiades Publishing, Russia 4 (2010) 1–11.

[17] G.J. Flynn, L.P. Keller, M.A. Miller, FTIR detection of organic of organic carbon in interplanetary particles, in: 29th Annual Lunar and Planetary Science Conference, 1998, Houston, TX, Abstract no. 1157.

[18] A.B. Paterakis, M. Steiger, The influence of conservation treatments and environmental storage factors on corrosion of copper alloys in the ancient Athenian Agora, Stud. Conserv. 2 (2003) 313–339.

[19] M. Khayet, T. Matsuura, J.I. Mengual, M. Qtaishat, Design of novel direct contact membrane distillation membranes, Desalination 192 (2006) 105–111.

[20] S.R. Krajewski, W. Kujawski, M. Bukowska, C. Picard, A. Larbot, Application of fluoroalkylsilanes (FAS) grafted ceramic membranes in membrane distillation process of NaCl solutions, J. Membr. Sci 281 (2006) 253–259.

[21] Z. Jin, D.L. Yang, S.H. Zhang, X.G. Jian, Hydrophobic modification of poly(phthalazinone ether sulfone ketone) hollow fiber membrane for vacuum membrane distillation, J. Membr. Sci 310 (2008) 20–27.

[22] J.R. McCutcheon, R.L. McGinnis, M. Elimelech, A novel ammonia—Carbon dioxide forward (direct) osmosis desalination process, Desalination 174 (2005) 1–11.